Catalysis Letters Vol. 112, Nos. 1–2, November 2006 (© 2006)
DOI: 10.1007/s10562-006-0161-4

Low temperature selective catalytic reduction of NO by NH_3 over V_2O_5 supported on TiO_2–SiO_2–MoO_3

Motonobu Kobayashi,* Ryoji Kuma, and Atushi Morita

Catalyst Research Laboratory, Nippon Shokubai Co., Ltd., 992-1 Okihama, Aboshi-ku, Himeji, Hyogo, 671-1292, Japan

Received 7 August 2006; accepted 19 September 2006

The V_2O_5 catalysts supported on TiO_2–SiO_2–MoO_3 (TSM) prepared by the coprecipitation method were investigated for the selective catalytic reduction (SCR) of NO by NH_3 at low temperatures. The V_2O_5/TSM catalyst with 7–13 wt% SiO_2 was found to exhibit a superior SCR activity and a good sulfur tolerance at low temperatures (<250 °C). The presence of highly active polymeric vanadates formed by the incorporation of MoO_3 to TiO_2–SiO_2 and superior redox properties seems to enhance SCR activity, and furthermore the very lower SO_2 oxidation activity due to the higher acidity leads to the remarkable improvement of sulfur tolerance.

KEY WORDS: TiO_2–SiO_2–MoO_3; V_2O_5/TiO_2–SiO_2–MoO_3; low temperature SCR; SO_2 oxidation; sulfur tolerance.

1. Introduction

The selective catalytic reduction (SCR) process, in which the NOx (NO, NO_2) are removed from flue gas by SCR of NO by ammonia is the most widespread technology for industrial flue gas treatment in stationary sources [1].

As commercial catalysts for the SCR process, vanadia catalysts supported on titania mixed with WO_3 or MoO_3 have been widely employed due to their high activity for the NOx removal reaction and good resistance against SOx poisoning [2–6]. In the application to flue gases from power plants, the SCR reactor is generally located upstream of the desulfurizer and electrostatic precipitator and is operated in the high temperatures range of 300–400 °C to avoid a catalyst deactivation due to pore plugging caused by the deposition of deactivating agents, ammonium salts such as NH_4HSO_4 and $(NH_4)_2SO_4$ on the catalyst surface [1,2].

However, the reduction of NOx by NH_3 in tail-end gases, i.e. flue gases from desulfurizer in power generation units, waste incinerators and other thermal processes is desirable to be performed at lower temperature below 200 °C in order to minimize energy consumption for reheating flue gases. Therefore, for commercial use, any catalysts employed for the low-temperature SCR process should be highly resistant to poisoning caused by SOx present in flue gases. It is well known [7,8] that SOx poisoning at low temperatures is due to deactivating agents, ammonium salts produced by the reaction of SO_3 generated from the oxidation of SO_2 with ammonia over the SCR catalyst. Therefore, the inhibition of the oxidation of SO_2 to SO_3 plays a critical role in the improvement of resistance to SOx poisoning at lower temperatures.

Various types of catalysts, i.e. $NiSO_4/Al_2O_3$ [9], $MnOx/A1_2O_3$ [10], MnOx–FeOx/TiO_2 [11], CuO–NiO/TiO_2 [12], Cu-exchanged mordenite [13] and V_2O_5/activated carbon [14] have been studied for the low-temperature SCR reaction. These catalysts exhibit comparatively high SCR activities at low temperatures below 200 °C, but there are few studies on the low-temperature SCR reaction in the presence of SOx, where the sulfur tolerance of the catalyst is a key point for industrial use. Thus, there have been still strong interests to develop highly active SCR catalysts with good sulfur tolerance at lower temperatures. More recently, it has been reported in our previous study [15,16] that V_2O_5 and V_2O_5–WO_3 catalysts supported on Ti-rich TiO_2–SiO_2 mixed oxide are highly active in the SCR reaction and simultaneously, less active in the SO_2 oxidation reaction. We have investigated the improvement of TiO_2–SiO_2-based mixed oxide as a support of vanadia catalysts in attempt to develop excellent low-temperature SCR catalysts.

The present work is to study the reactivity and sulfur tolerance of V_2O_5 catalysts supported on TiO_2–SiO_2–MoO_3 (TSM) in the SCR reaction at low temperatures. For this purpose, V_2O_5 catalysts supported on TSM with various compositions were prepared and characterized by BET, XRD, Raman and NH_3–TPR. The results are compared with a commercial catalyst, V_2O_5–MoO_3/TiO_2 catalyst.

---

*To whom correspondence should be addressed.

1011-372X/06/1100–0037/0 © 2006 Springer Science+Business Media, Inc.

2. Experimental

2.1. Catalyst preparation

The TSM mixed oxide with different compositions were prepared by cop-recipitaion of the mixed solution of titanyl sulfate, silica sol and ammonium molybdate with an aqueous ammonia. After the resultant mixture was aged at 30 ~ 40 °C for 10 h, the precipitate was separated by filtration, washed thoroughly with distilled water, and dried at 150 °C for 10 h, followed by the calcination at 500 °C for 3 h in an atmosphere of air and by the pulverization with a hammer mill. TiO_2–SiO_2 and TiO_2 was also prepared similarly as above.

An appropriate amount of ammonium metavanadate was dissolved in a mixed aqueous solution of monoethanol amine and oxalic acid (ammonium metavanadate:oxalic acid:monoethanol amine = 1:1:0.8 weight ratio) at room temperature. This solution and TSM powders obtained above were thoroughly mixed under continuous addition of suitable amounts of water and kneaded. The resultant blend was molded with an extrusion molding device to produce a honeycomb monolith with 50 mm × 50 mm in outer diameter, mesh of 3.2 mm and 300 mm in length. The obtained monolith was dried at 60 °C, and then calcined under the current of air at 450 °C for 5 h. Thus, the V_2O_5/TiO_2–SiO_2–MoO_3 catalysts with different contents of V_2O_5, MoO_3 and SiO_2 were obtained. For comparison, the V_2O_5–MoO_3/TiO_2–SiO_2 and the V_2O_5–MoO_3/TiO_2 catalysts were prepared in the same way as in the above preparation by using the above TiO_2–SiO_2 and TiO_2 powders, respectively and a mixed aqueous solution of ammonium metavanadate and ammonium molybdate.

For the support designation, TSM and TiO_2–SiO_2 are denoted as TSM and TS, respectively. The number before S and M indicates the contents of SiO_2 and MoO_3 (wt%), respectively. Namely, T7S10M shows the contents of 7 wt% SiO_2 and 10 wt% MoO_3.

2.2. Characterization of catalysts

X-ray diffraction measurement for supports and catalysts was carried out by a Spectris diffractometer with a CuK_α. BET surface area was measured by the BET method using a Yuasa Ionics-4-SORB apparatus.

Temperature programed desorption experiments with NH_3 (NH_3–TPD) were carried out by a Bell Japan Automatic temperature programed desorption spectrometer as follows. The powdered samples were placed inside reactor and preheated in flowing air at 450 °C for 1 h and cooled to 150 °C. Then a stream of 0.2% NH_3 in He was fed to the reactor and then the samples were heated to 500 °C under the same flow at 10 °C/min.

In situ Raman spectra were measured with a Almega-Raman spectrometry (Themo Electric Corporation). The samples pressed into self-supporting wafers (no KBr) were cooled down to 80 °C after heating at 500 °C for 1 h in air and at this temperature the *in situ* Raman spectra were recorded.

2.3. Catalytic activity measurement

The catalytic activity measurement for the SCR reaction of NO by NH_3 was carried out in a fixed bed reactor made of a stainless steel tube with 1.5 inch in inside diameter. The testing honeycomb catalysts cut out to a size of 4 × 4 cells were loaded in the reactor. The reaction gas mixture which consisted of 200 ppm NO, 200 ppm NH_3, 10% O_2 by volume and 10% H_2O by volume with N_2 as the carrier gas was fed into the reactor. The total flow through the reactor was 1.0 Nm^3/h and a gas hourly space velocity (GHSV) was 11,000 h^{-1}. The concentration of NO was analyzed by on-line chemiluminescence NOx analyzer.

The SO_2 oxidation experiment was conducted using the same apparatus as in the SCR experiment at GHSV of 6,000 h^{-1} with 150 ppm of SO_2 feed concentration. The SO_2 oxidation activity was measured after the aging of more than 60 h until the amount of sulfate on the catalyst formed by the oxidation of SO_2 reaches to an equilibrium state.

The SO_2 conversion was determined by measuring the SO_3 concentration in the outlet gas stream. SO_3 was condensed as a sulfuric acid in a collector with a glass filter at 90 °C, followed by the titration with barium acetate using arsenazo(III) as indicators in order to determine the SO_3 concentration [17].

3. Results and discussion

3.1. Characterization of TSM supports and V_2O_5/TSM catalysts

The BET surface areas of TSM supports with different compositions and the corresponding vanadia catalysts are summarized in table 1. TSM and V_2O_5/TSM catalysts are found to exhibit remarkably large surface areas (135 and 101 m^2/g, respectively) as compared to TiO_2 and V_2O_5–MoO_3/TiO_2 reference catalyst (82 and 60 m^2/g, respectively). The addition of V_2O_5 to TSM decreases the surface area of the catalyst.

With increasing the SiO_2 content in TSM, the surface areas of TSM with the same MoO_3 content (10 wt%) increase significantly, i.e. they are 82, 135, 151, 168 and 174 m^2/g when the SiO_2 contents are 0, 7, 13, 20 and 30 wt%, respectively and those of the corresponding catalysts also increase as well.

The XRD patterns of TSM supports and V_2O_5/TSM catalysts are shown in figure 1 as compared with a V_2O_5–MoO_3/TiO_2 reference catalyst. It is apparently observed that the crystallinity of anatase TiO_2 (peak at $2\theta = 25.3°$) is lower for V_2O_5/TSM than for V_2O_5–MoO_3/TiO_2 and it decreases with increasing SiO_2 content in TSM. In contrast, the addition of MoO_3 to TS

Table 1
BET surface areas of TSM with different compositions and 8 wt% V_2O_5/TSM catalysts

Compositions of TSM (wt%)				BET surface area (m^2/g)	
TiO_2	SiO_2	MoO_3		TSM	8 wt%V_2O_5/TSM
93	7	0	(TS)	163	120[a]
93	7	0	(TS)	163	111[b]
88	7	5		158	105
83	7	10		135	101
78	7	15		126	95
77	13	10		151	118
70	20	10		168	131
60	30	10		174	142
100	0	0	(TiO_2)	82	60[c]

[a] For 8 wt%V_2O_5/TS.

[b] For 8 wt%V_2O_5-10 wt%MoO_3/TS.

[c] For the reference catalyst (8 wt%V_2O_5-10 wt%MoO_3/TiO_2). TSM and V_2O_5/TSM were calcined under the current of air at 500 and 450 °C, respectively.

slightly promotes the growth of crystalline titania phase in TS and V_2O_5/TS. In all catalyst samples, no visible crystal phase of V_2O_5 (peaks at $2\theta = 20.3$, 26.1 and 31.0°) and MoO_3 (peaks at $2\theta = 25.8$, 23.6 and 39.0°) cannot be detected. This reveals that vanadia is highly dispersed on TSM, possibly due to a large surface area of TSM.

The surface structures of V_2O_5/TSM, V_2O_5/TS, V_2O_5–MoO_3/TS and TSM were examined by Raman spectroscopy as compared to those on V_2O_5/TiO_2 and V_2O_5–MoO_3/TiO_2. These results are shown in figure 2. Two major peaks are observed near 1030 and 994 cm^{-1} of Raman shift, and broad peaks appear at 920–960 cm^{-1}. The sharp peaks near 1030 cm^{-1} are observed for V_2O_5 catalysts and commonly assigned to monomeric vanadyl species [18,19]. The small peaks near 994 cm^{-1} and very weak peaks near 970 cm^{-1} observed for TSM correspond to crystalline MoO_3 and the M = O stretching mode of molybdenyl species, respectively [20,21]. The phase of crystalline MoO_3 has not been detected in the XRD spectra due to the low sensibility of XRD, thereby not applicable to small crystallites less than 4 nm in diameter. The broad peaks at 920–960 cm^{-1} are generally recognized to be assigned to polymeric vanadate species, although the base line is changed [18,19].

As shown in figure 2, monomeric vanadyl species and polymeric vanadate species are apparently formed on the catalyst surfaces of both V_2O_5/TiO_2 and V_2O_5–MoO_3/TiO_2 and are also observed for V_2O_5/TSM. For V_2O_5/TS and V_2O_5–MoO_3/TS, however, monomeric vanadyl species are observed, but polymeric vanadate species are not observed. These results indicate that the incorporation of MoO_3 to TS by the coprepicitation method rather than the impregnation method enhances the formation of polymeric vanadate species.

Such a promotion effect by MoO_3 seems to be possibly due to that the available surface sites for vanadia according to the preoccupation of surface sites by MoO_3 are reduced, as pointed out in the study reported by

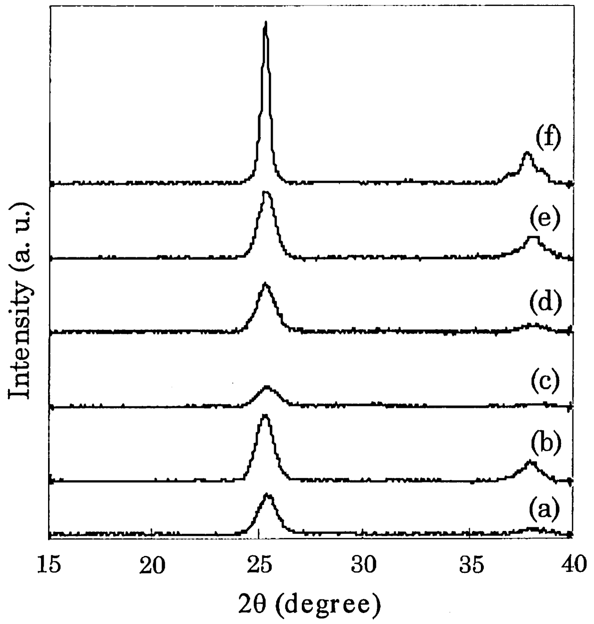

Figure 1. XRD patterns of supports and V_2O_5 catalysts: (a) T7S, (b) T7S10M, (c) T20S10M, (d) 8 wt% V_2O_5/T8S, (e) 8 wt% V_2O_5/T7S10M and (f) 8 wt% V_2O_5-10 wt% MoO_3/TiO_2 (reference catalyst).

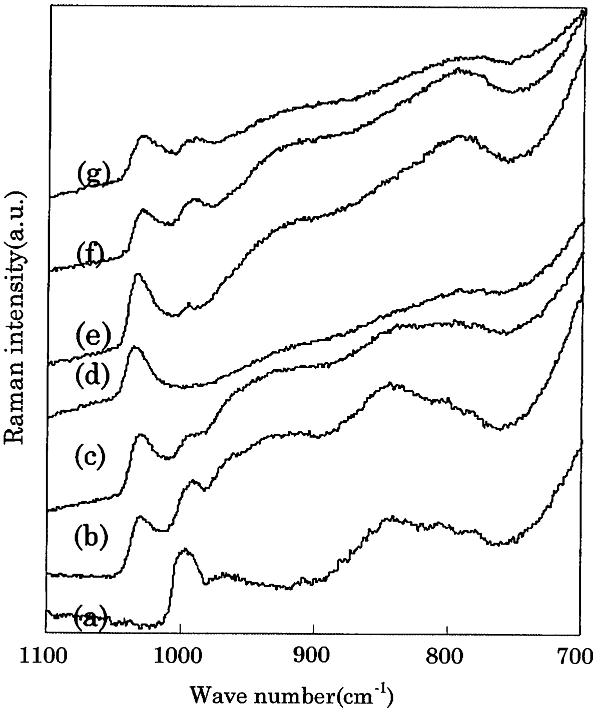

Figure 2. Raman spectra of supports and V_2O_5 catalysts: (a) T7S10M, (b) 4 wt% V_2O_5/T7S10M, (c) 8 wt% V_2O_5/T7S10M, (d) 8 wt% V_2O_5/T7S, (e) 8 wt% V_2O_5/TiO_2, (f) 8 wt% V_2O_5-10 wt% MoO_3/TiO_2 and (g) 8 wt% V_2O_5-10 wt% MoO_3/TS.

Choo *et al.* [22] that WO_3 promotes the formation of polymeric vanadate species present on the surface of V_2O_5/TiO_2. It is worth noting that the incorporation of MoO_3 to TS by the coprepicitation method promotes the formation of polymeric vanadate species.

In V_2O_5/TSM, the characteristic peaks of crystalline V_2O_5 are not observed in the XRD and Raman spectra. This suggests that vanadia species on the surface of TSM are present in the form of highly dispersed monomeric vanadyl species and polymeric vanadate species.

In order to study the acidity and reducibility of V_2O_5/TSM and V_2O_5–MoO_3/TS, temperature programed desorption of ammonia (NH_3–TPD) experiments were performed and compared with the V_2O_5–MoO_3/TiO_2 catalyst with the same V_2O_5 and MoO_3 contents. The features of NH_3–TPD spectra with the desorption of NH_3 and the evolution of small amounts of N_2 are shown in figures 3 and 4, respectively.

As shown in figure 3, the acidities of V_2O_5/TSM and V_2O_5–MoO_3/TS are observed to be nearly the same, while they are higher than those of V_2O_5–MoO_3/TiO_2.

On the other hand, it is seen in figure 4 that the formation of N_2 is observed with increasing temperatures regardless of the absence of oxygen in a gas stream, which thus indicates that NH_3 adsorbed on the catalyst surface reacts with catalyst lattice oxygen to selectively produce N_2 as follows:

$$2\,NH_3 + 3O^{2-} \rightarrow 2N_2\ 3H_2O\ +\ 6e^-$$

where O^{2-} is a catalyst lattice oxygen ion. In this case, NH_3 acts as a reducing agent and N_2 formation is indicative of catalyst reduction.

As shown in figure 4, it is apparently found that the incline of the NH_3–TPD traces after the N_2 formation starts is higher for V_2O_5/TSM than for V_2O_5–MoO_3/TiO_2. This indicates that the rate of N_2 formation is faster over V_2O_5/TSM than over V_2O_5–MoO_3/TiO_2 at low temperatures, suggesting that V_2O_5/TSM is more easily reduced by NH_3 than V_2O_5–MoO_3/TiO_2. Therefore, the V_2O_5/TSM catalyst exhibits a superior redox ability of vanadium oxide as compared with the V_2O_5–MoO_3/TiO_2 catalyst.

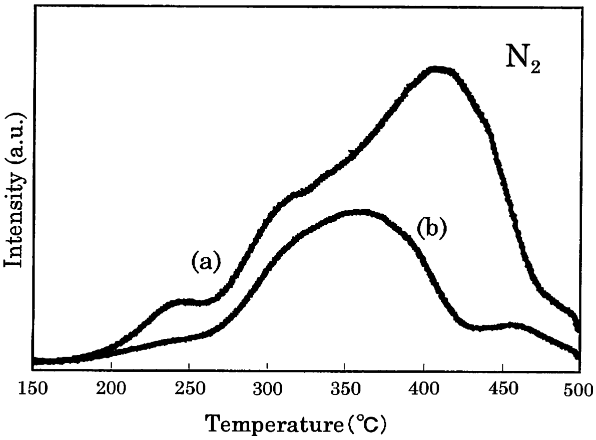

Figure 4. NH_3–TPR spectra of (a) 8 wt%V_2O_5/T7S10M and (b) 8 wt%V_2O_5-10 wt% MoO_3/TiO_2; N_2 concentration as a function of temperature. V_2O_5, MoO_3 and SiO_2 contents are 8, 10 and 7 wt%, respctively.

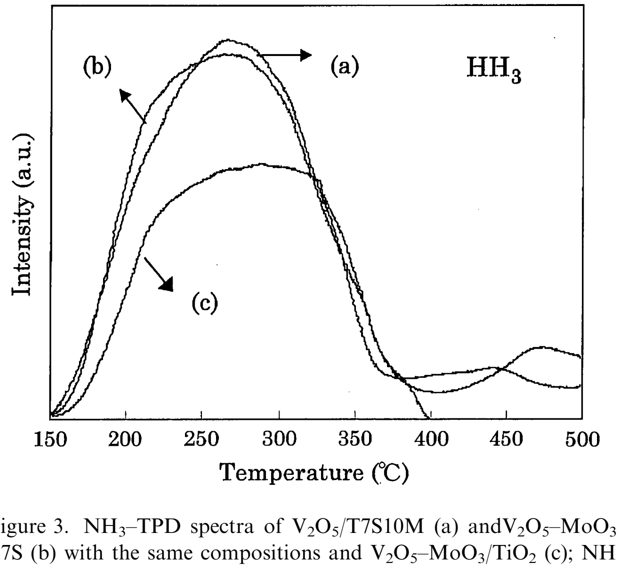

Figure 3. NH_3–TPD spectra of V_2O_5/T7S10M (a) andV_2O_5–MoO_3/T7S (b) with the same compositions and V_2O_5–MoO_3/TiO_2 (c); NH_3 concentration as a function of temperature. V_2O_5, MoO_3 and SiO_2 contents are 8, 10 and 7 wt%, respectively.

3.2. *Effect of V_2O_5 loading and compositions of TSM on SCR activity*

The effect of V_2O_5 loading on the SCR activity was examined over the V_2O_5/TSM catalyst. As shown in figure 5, NO conversion significantly increases with increasing the V_2O_5 loading, particularly at low temperatures less than 250 °C and shows a maximum near a loading of 8 wt%. A further increase in the V_2O_5

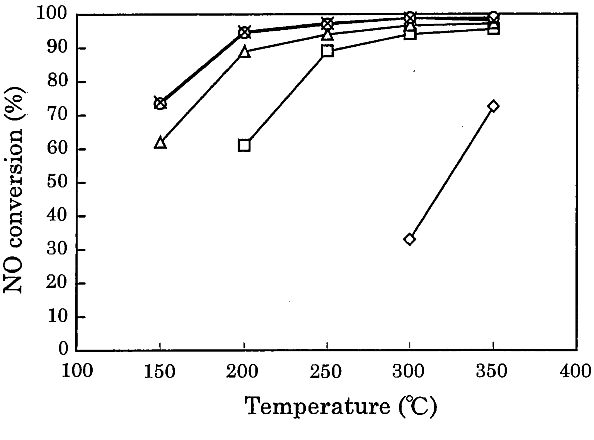

Figure 5. SCR activity of V_2O_5/TSM with V_2O_5 loadings of 0 (◇), 2 (□), 4 (△), 8(○) and 12 wt% (×). SiO_2 contents are all 7 wt%. Reaction conditions: 200 ppm NO, 200 ppm NH_3, 10 vol% O_2, 10 vol% H_2O, N_2 balance. SV: 11,000 h^{-1}.

loading does not result in a further increase in NO conversion.

The effect of MoO_3 and SiO_2 contents in TSM prepared by coprecipitation method on the SCR activity has been investigated with respect to 8 wt% V_2O_5-based catalyst where the highest SCR activity are obtained.

Figure 6 shows the results of SCR activity tests over the V_2O_5 TSM catalysts with different MoO_3 contents (0, 5 and 15 wt%). With increasing the MoO_3 content, the SCR activity increases significantly, particularly at low temperatures below 250 °C and reaches a nearly maximum at a MoO_3 content of 10 wt%. The V_2O_5/TSM catalysts shows a remarkably improved SCR activity.

In figure 7, the SCR activity of V_2O_5/TSM and V_2O_5–MoO_3/TS with the same compositions prepared by different preparations is shown in comparison with the commercial catalyst, V_2O_5–MoO_3/TiO_2 with the same V_2O_5 and MoO_3 contents. The SCR activity increases in the order of $V_2O_5\text{–}MoO_3/TiO_2 < V_2O_5\text{–}MoO_3/TS \ll V_2O_5/TSM$, apparently indicating that V_2O_5 supported on TSM prepared by the coprecipitation method exhibits a much higher SCR activity than V_2O_5–MoO_3 supported on TS in spite of the same composition.

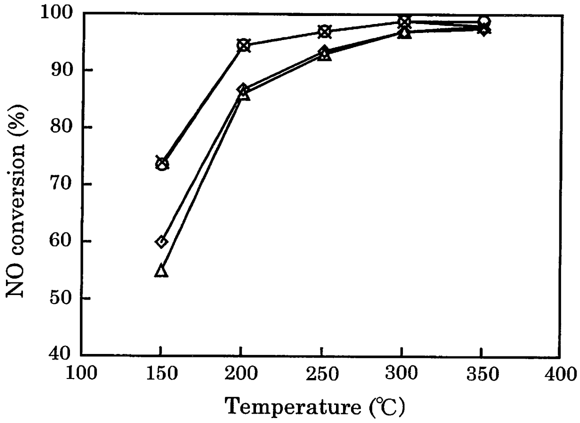

Figure 6. SCR activity of 8 wt% V_2O_5/TSM catalysts with SiO_2 contents of 0 (◇), 7 (○), 13 (△), 20 (×) and 30% wt% (□). MoO_3 content in TSM are all 10 wt%. Reaction conditions: 200 ppm NO, 200 ppm NH_3, 10 vol% O_2, 10 vol% H_2O, N_2 balance. SV: 11,000 h^{-1}.

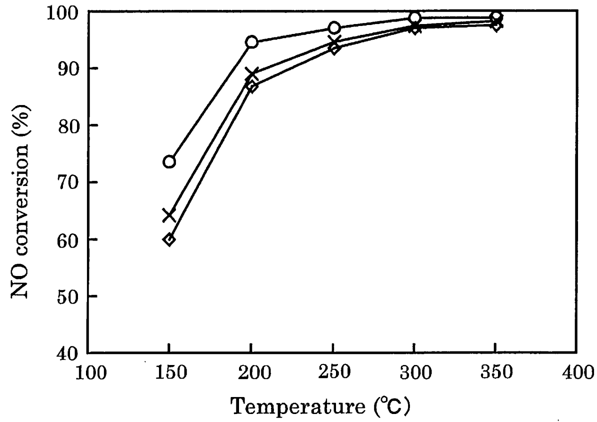

Figure 7. SCR activity of V_2O_5/TSM (○) and V_2O_5–MoO_3/TS (×) with the same compositions and V_2O_5–MoO_3/TiO_2 (◇). V_2O_5, MoO_3 and SiO_2 contents are all 8, 10 and 7 wt%, respectively. Reaction conditions: 200 ppm NO, 200 ppm NH_3, 10 vol% O_2, 10 vol% H_2O, N_2 balance. SV: 11,000 h^{-1}.

Different several mechanisms of the SCR reaction on V_2O_5/TiO_2 have been proposed [23,24]. It is certain that the mechanism can be described by the following steps, involving a surface redox site adjacent to a surface acid site.

$$NH_3 + a \rightarrow NH_3 - a \text{ (a: acid site)} \quad (1)$$

$$NH_3 - a + O - \text{(lattice)} \rightarrow NH_2 - a + HO - \text{(lattice)} \quad (2)$$

$$NH_2 - a + NO \rightarrow N_2 + H_2O \quad (3)$$

$$HO - \text{(lattice)} + O_2 \rightarrow O - \text{(lattice)} \quad (4)$$

The first step (reaction (1)) in SCR is the adsorption of ammonia at acid sites, followed by the activation of ammonia (reaction (2)), which occurs via reaction with surface oxygen or lattice oxygen present in $V = O$ groups. The gaseous NO reacts with activated ammonia and then N_2 and H_2O are formed (reaction (3)). Reduced vanadium oxide is reoxidized by gaseous oxygen (reaction (4)). This mechanism indicates that the combination of adsorption sites (acid sites) and activation sites (vanadium oxide) are one of the major controlling factors in the SCR reaction. Thus, both acidities and redox properties of the catalyst control the reactivity.

It has been reported for V_2O_5/TiO_2 [18,25] that the specific SCR activity of the polymeric vanadate species is about 10 times greater than that of monomeric vanadyl species on the catalyst surface at 500 K. The greater reactivity of polymeric vanadate species as the activation site is related to the greater lability of lattice oxygen atoms, which results in faster reduction by NH_3 and faster reoxidation by gaseous oxygen, implying higher redox properties. Choo *et al.* [26] also reported that the formation of polymeric vanadate species particularly improves the SCR activity at low temperatures. Therefore, the activity at low temperatures depends on the redox ability of the catalyst, while acid sites play a key role in controlling the activity at high temperatures [27].

As seen in Raman spectra (figure 2), polymeric vanadate species are present on V_2O_5/TSM but almost absent on both V_2O_5/TS and V_2O_5–MoO_3/TS, clearly indicating that MoO_3in TSM promotes the formation of polymeric vanadate species.

On the other hand, as demonstrated by NH_3–TPD spectra in figure 3, V_2O_5/TSM exhibits almost the same acidity as V_2O_5–MoO_3/TS. Furthermore, as listed in table 1, the surface area is smaller for V_2O_5/TSM than for V_2O_5–MoO_3/TS. As a result, the higher activity for V_2O_5/TSM than for V_2O_5–MoO_3/TS cannot be explained by the difference in the acidity and surface area of the catalyst. Therefore, the enhanced activity of V_2O_5/TSM at low temperatures seems to be mainly attributed to the formation of highly active polymeric vanadate species induced by the incorporation of MoO_3 to TS by the coprecipitation method

As seen in figure 7, the V_2O_5/TSM catalyst exhibits a superior activity in the low temperature region as compared with the commercial V_2O_5–MoO_3/TiO_2 catalyst with the same content of V_2O_5 (8 wt%) and MoO_3 (10 wt%). The higher reactivity of V_2O_5/TSM seems to related to its superior redox property, which is demonstrated by NH_3–TPD experiments with the evolution of N_2 (figure 4).

In fact, it has been reported that the superior redox property of V_2O_5–MoO_3/TiO_2 is related to the existence of a V–Mo electronic interaction operating through the TiO_2 support, which leads to the higher SCR activity [28]. Therefore, the higher reducibility observed for V_2O_5/TSM may be attributed to that the electronic interaction between V and Mo species and supports operates more strongly via TSM than via TiO_2.

Figure 8 shows the effect of SiO_2 content in TSM on the SCR activity of the V_2O_5/TSM catalysts having the same contents of V_2O_5 (8 wt%) and MoO_3 (10 wt%). The NO conversion increases with SiO_2 content and reaches a maximum at the SiO_2 contents of 7–13 wt% and then decreases. Such an effect of SiO_2 on the SCR activity is observed in the whole measured temperature range. Similar trends have been reported on the V_2O_5/TS catalyst in our previous study [15] that in V_2O_5/TS catalyst containing no MoO_3, the incorporation of SiO_2 of 10–20 mol% (7.7–15.8 wt%) to TiO_2 by the coprecipitation method improves the SCR activity and it is associated with highly dispersed vanadia due to a large surface area and more controlled acidities and acid strengths. Therefore, the effect of SiO_2 in the case of the V_2O_5/TSM catalyst also seems to come from the same reason (large surface areas and optimized acidities) as in the case of the above V_2O_5/TS catalyst.

3.3. *Effect of compositions of TSM on SO_2 oxidation activity*

The activity in the oxidation of SO_2 to SO_3 over the V_2O_5/TSM catalysts with different contents of MoO_3 and SiO_2 was examined at a reaction temperature of 250 °C. Figure 8 shows the effect of SiO_2 content in TSM on the SO_2 oxidation activity of V_2O_5/TSM with the same V_2O_5 and MoO_3 contents. The SO_2 oxidation activity is found to be largely affected by the SiO_2 content in TSM, showing that with increasing the SiO_2 content, the SO_2 conversion significantly decreases. At SiO_2 contents of 7–13 wt%, which exhibit a highest SCR activity, the SO_2 conversion is roughly a third that of V_2O_5–MoO_3/TiO_2.

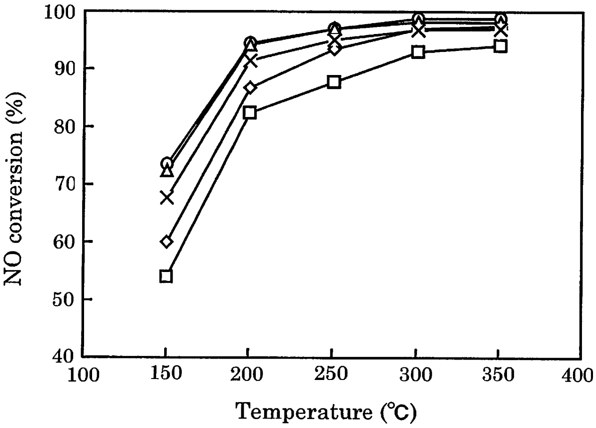

Figure 8. SCR activity of 8 wt% V_2O_5/TSM with SiO_2 contents of 0 (◇), 7 (○), 13 (△), 20 (×) and 30% wt% (□). MoO_3 contents are all 10 wt%. Reaction conditions: 200 ppm NO, 200 ppm NH_3, 10 vol% O_2, 10 vol% H_2O, N_2 balance. SV: 11,000 h^{-1}.

Similar effects of SiO_2 on the SO_2 oxidation activity has been observed for the V_2O_5/TS catalyst in our previous study [15] and it was reported that the incorporation of SiO_2 to TiO_2 by the coprecipitation method significantly decreases the SO_2 oxidation activity due to the lower oxidation state of vanadium species induced by the increase in acidity of the TS support. Therefore, the remarkably lower SO_2 oxidation activity of V_2O_5/TSM, as compared with V_2O_5–MoO_3/TiO_2, seems to be related to the higher acidity as shown in figure 3. Such an effect of SiO_2 on SO_2 oxidation activity for V_2O_5/TSM is in good agreement with that for V_2O_5/TS.

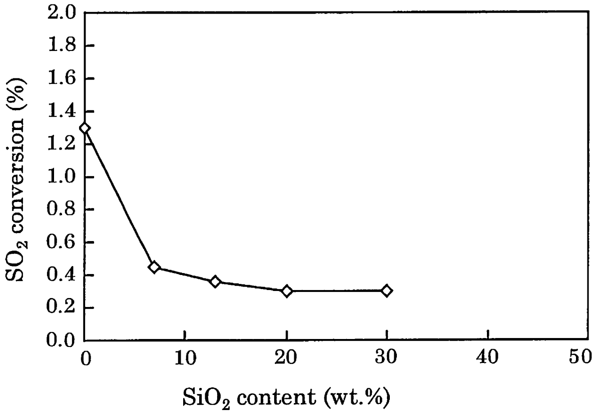

Figure 9. Effect of SiO_2 content on SO_2 oxidation activity over 8 wt% V_2O_5/TSM at 250 °C. MoO_3 contents are all 10 wt%. Reaction conditions: 150 ppm SO_2, 10 vol% O_2, 10 vol% H_2O, N_2 balance. SV: 6,000 h^{-1}.

Figure 9 shows the SO_2 conversion as a function of MoO_3 content in TSM. It is apparently observed that the increase in MoO_3 content slightly enhances the SO_2 oxidation activity.

Similar promoting effect of MoO_3 on the SO_2 oxidation activity has been observed for the V_2O_5/TiO_2 catalyst [8]. The improvement of SO_2 oxidation activity by the incorporation of MoO_3 to TS by the coprecipitation method seems be related to the formation of polymeric vanadate species which are responsible for the oxidation of SO_2 as well as for the oxidation of NH_3 [16].

It is worth noting that the V_2O_5/TSM catalyst exhibits a remarkably lower activity for the oxidation of SO_2 than the commercial V_2O_5–MoO_3/TiO_2 catalyst with the same V_2O_5 and MoO_3 contents.

3.4. Sulfur tolerance of V_2O_5/TSM catalysts

The sulfur tolerance experiment of the V_2O_5/TSM catalysts was conducted by evaluating the SCR activity at NH_3/NO molar ratio of 1.0 after the SCR reaction took place at NH_3/NO molar ratio of 0.8 with 150 ppm of SO_2 feed concentration at a lower temperature of 175 °C. The results are shown in figure 10 as compared with a V_2O_5–MoO_3/TiO_2 catalyst (figure 11). The decrease in the SCR activity during a 400 h-operation is found to be remarkably lower for both V_2O_5/T7S10M and V_2O_5/T20S10M than V_2O_5–MoO_3/TiO_2 with the same contents of V_2O_5 (8 wt%) and MoO_3 (10 wt%). This seems to be related to the major difference in the SO_2 oxidation activity of the catalysts as shown in figure 9.

It is well known [7,8] that the deactivation of SCR catalysts in the presence of SO_2 at low temperatures is primarily due to the blocking and filling of catalyst pores caused by the formation of ammonium sulfate compounds such as $(NH_4)_2SO_4$ and NH_4HSO_4 on the catalyst. Since these ammonium salts are formed by an equilibrium reaction among NH_3, SO_3 and H_2O, the higher concentrations of NH_3 and SO_3 and lower temperatures favor the formation of these ammonium salts. This indicates that the lower activity of SO_2 oxidation to SO_3 leads to a superior sulfur tolerance of the catalyst at low temperatures. Therefore, the higher sulfur tolerance observed for V_2O_5/TSM are attributed to a significantly low SO_2 oxidation activity as compared with the V_2O_5–MoO_3/TiO_2 as shown in figure 9.

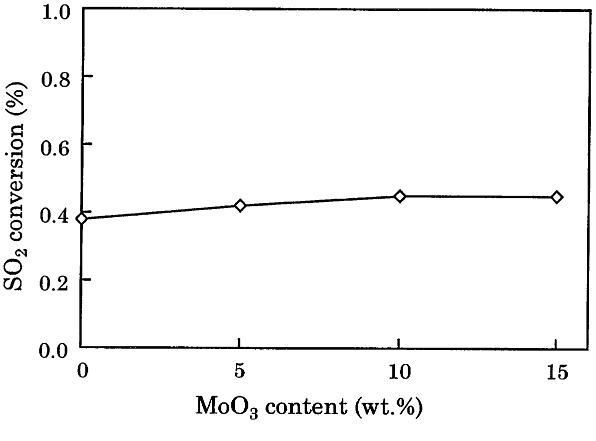

Figure 10. Effect of MoO_3 content on SO_2 oxidation activity over 8 wt% V_2O_5/TSM at 250 °C. SiO_2 contents are all 7 wt%. Reaction conditions: 150 ppm SO_2, 10 vol% O_2, 10 vol% H_2O, N_2 balance. SV: 11,000 h^{-1}.

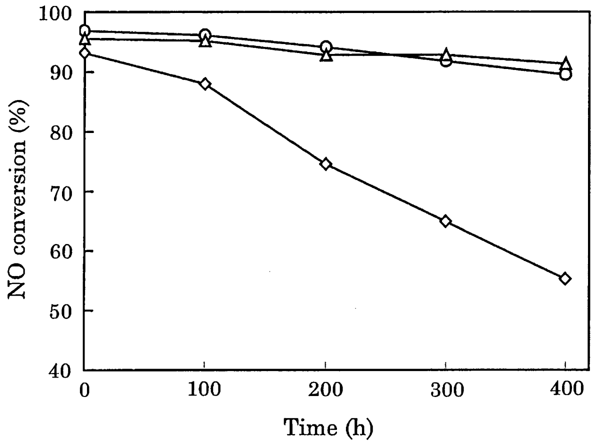

Figure 11. Sulfur tolerance of V_2O_5/TSM and V_2O_5–MoO_3/TiO_2 at 175 °C: (○) 8 wt% V_2O_5/T7S10M, (△) 8 wt% V_2O_5/T20S10M and (◇) 8 wt% V_2O_5–10 wt% MoO_3/TiO_2. Reaction conditions: 100 ppm NO, 80 ppm NH_3,150 ppm SO_2, 10 vol% O_2, 10 vol% H_2O, N_2 balance. SV: 6,000 h^{-1}. NO conversion was measured at NH_3/NO molar ratio of 1.0.

4. Conclusions

The following conclusions have been drawn from the present study.

(1) The V_2O_5 catalyst supported on TSM with 7–13 wt% SiO_2, prepared by the coprecipitation method is found to exhibit a superior SCR activity, and a good sulfur tolerance at lower temperatures (<250 °C) as compared with the commercial V_2O_5–MoO_3/TiO_2 catalyst with the same V_2O_5 (8 wt%) and MoO_3 (10 wt%) contents. Such more superior SCR activity at lower temperatures seems to be mainly attributed to the presence of polymeric vanadate species and higher redox properties besides higher surface areas.

(2) The incorporation of MoO_3 to TS is found to promotes the formation of polymeric vanadate species, resulting in the remarkable enhancement of the SCR activity.

(3) TSM and V_2O_5/TSM exhibit large surface areas (ca. 100 m^2/g) and very lower crystalline anatase TiO_2, thus suggesting that vanadia is highly dispersed on TSM as demonstrated by XRD and Raman analysis.

(4) The SO_2 oxidation activity is found to be significantly suppressed with increasing the SiO_2 content in TSM. The very lower SO_2 oxidation activity of the V_2O_5/TSM catalyst due to its higher acidity leads to the remarkable improvement of sulfur tolerance of the V_2O_5/TSM catalyst at low temperatures, which is a very important key factor for industrial applications to low-temperature SCR processes.

References

[1] H. Bosch and F. Janssen, Catal. Today 2 (1988) 369.
[2] F. Nakajima and I. Hamada, Catal. Today 29 (1996) 109.
[3] J.P. Chen and R.T. Yang, Appl. Catal. A 80 (1992) 135.
[4] L.J. Alemany, L.J. Lietti, N. Ferlazzo, P. Forzatti, G. Busca, E. Giamello and F. Bregani, J. Catal. 155 (1995) 117.
[5] S. Morikawa, H. Yoshida and K.Takahashi, Chem. Lett. (1981) 251.
[6] L. Casagrande, L. Lietti, I. Nova, P. Forzatti and A. Baiker, Appl. Catal. B (1999) 63.
[7] S. Matsuda, T. Kamo, A. Kato and F. Nakajima, Ind. Eng. Chem. Prod. Res. Dev 21 (1982) 42.
[8] S.W. Ham, H. Choi, I.S. Nam and Y.G. Kim, Ind. Chem. Res 34 (1995) 1616.
[9] J.P. Chen, R.T. Yang, M.A. Buzanowski and J.E. Cichanowicz, Ind. Eng. Chem. Res 29 (1990) 1431.
[10] L. Singoredjo, R. Korver and F. Kapteijin, J. Moujlijin, Appl. Catal. B 1 (1992) 297.
[11] G. Qi and R.T. Yang, Appl. Catal. B 44 (2003) 217.
[12] G. Blanco, P. Avila, S. Suárez, J.A. Martín and C. Knapp, Appl. Catal. B 28 (2000) 235.
[13] S.W. Ham, H. Choi, I.S. Nam and Y.G. Kim, Ind. Eng. Chem. Res 34 (1995) 1616.
[14] Z. Zhu, Z. Liu, H. Niu and S. Liu, J. Catal 187 (1999) 245.
[15] M. Kobayashi, R. Kuma, S. Masaki and N. Sugishima, Appl. Catal. B 60 (2005) 177.
[16] M. Kobayashi and M. Hagi, Appl. Catal. B 63 (2005) 104.
[17] H. Goksøyr and K. Ross, J. Inst. Fuel 35 (1962) 177.
[18] G.T. Went, L. Leu, R.R. Rosin and A.T. Bell, J. Catal 134 (1992) 492.
[19] M. Vuurman and L. Wachs, J. Phys. Chem 95 (1991) 241.
[20] H. Miyata, S. Tokuda and T. Ono, J. Chem. Soc 86(12) (1990) 2291.
[21] L.E. Wachs, Catal. Today 27 (1996) 437.
[22] S.T. Choo, S.D. Yim, I.S. Nam, S.W. Ham and J.B. Lee, Appl. Catal B (2003) 237.
[23] G. Busca, L. Lietti, G. Ramis and Berti, Appl. Catal. B 18 (1998) 1.
[24] Topsøe, J. Catal 151 (1995) 241.
[25] Lietti, J. Catal 147 (1994) 241.
[26] S.T. Choo, Y.G. Lee, I.S. Nam, S.W. Ham and J.B. Lee, Appl. Catal. A 200 (2000) 177.
[27] P. Forzatti and L. Lietti, Heterogen. Chem. Rev 3 (1996) 33.
[28] L. Casagrande, L. Lietti, I. Nova, P. Forzatti and A. Baiker Appl. Catal. B (1999) 63.